Journal of Research Administration
Society of Research Administrators International

ANALYSIS OF THE OPTICAL CHARACTERISTICS OF POROUS SILICON AND POROUS SILICON MODIFIED WITH POLYMERS

Dr K Kulathuraan[a], Dr T Jayaprakash[b], Dr T Arivazhagan[c], Mrs V Ramyac, Mrs A Lakshmi Priya[d]

[a] Associate Professor in Physics, Arulmigu Palaniandavar College of Arts and Culture, Dindigul, India

[b] Professor in Physics, Nehru Institute of Technology, Coimbatore, India

[c] Associate Professors in Physics, Sri Sairam Institute of Technology, Chennai, India

[d] Assistant Professor (SG), Nehru Institute of Engineering and Technology, Coimbatore

pkkmaterials@gmail.com, nitjayaprakash@nehrucolleges.com

ABSTRACT

Crystalline, microcrystalline and amorphous silicon have been playing a very important role in many aspects of fundamental and applied research fields as a result of the well-established and relatively cheap technology of this semiconductor element. However, with an energy gap of 1.1 eV, silicon remained up till recently unapplied into optoelectronics, which was reserved to compound semiconductor technologies of which are relatively difficult and, usually, very costly. The discovery of the visible electroluminescent phenomenon in porous silicon (PS) even at room temperature stimulated a great deal of interest. With an energy gap of 0.5 eV greater than its crystalline counterpart, this semiconductor opened up many other application fields such as opto, micro, and nano-electronics. The chapter describes the theoretical calculation of optical properties of porous silicon and polymers treated porous silicon. The Optical properties of porous silicon and polymers treated porous silicon were also depending upon the porosity. It is concluded that the theoretical calculation is a simple way to confirm the experimental results.

Keywords: Porous Silicon (PS), Polymers treated porous silicon, Optical Properties, Etching time, PMMA & PVC Concentrations

1. INTRODUCTION

Young's modulus, Poisson's ratio, shear modulus, and bulk modulus are material constants that describe mechanical characteristics and may have different values with respect to porosities. Therefore, to properly design devices composed of such silicon based anisotropic materials, and for which such mechanical properties are important, the mechanical properties of porous silicon are being investigated. The acoustic parameters that can be investigated are transverse, longitudinal, and Rayleigh velocities (VT, VL and VR respectively), longitudinal impedance (ZL) and transverse impedance (ZT). Several attempts concerning the dependence of porosity (P), on these acoustic parameters were previously reported in connection with some materials [1-3]. Hence, the investigation of porosity is of great importance in the determination of material characteristics, and the knowledge of elastic constants and related properties are indispensable for the application of electroluminescent devices. To this purpose, the elastic properties and acoustic properties of the porous silicon are of particular interest.

Since porous silicon is a mixture of silicon and air, the refractive index of porous silicon is expected to be lower than that of bulk silicon and is dependent upon the porosity of that particular layer. Obviously, as the ratio of silicon to air decreases that is as the porosity increases the refractive index of the PS also decreases. Many attempts have been made to relate the refractive index and the energy gap Eg through simple relationship [4-7]. However, these relationships of refractive index (n) are independent of temperature and incident photon energy. Ravindra and Srivastava [7] have suggested a linear form of n as a function of Eg,

$$n = \alpha + \beta\, Eg \quad (1)$$

where, α = 4.048 and β = -0.62 (eV)-1.

To understand the porosity and the energy gap dependence of the elastic properties of PS, will first say general features observed in theories for the elasticity of cellular materials. These theories are typically semi-empirical for PS, which retains its c-Si lattice structure in the solid skeleton around the pores, we show how the porosity dependence of the elastically can be incorporated into the representation of an anisotropic material. Many authors have made various efforts to explore thermodynamic properties of solids [8-12]. In these studies, the authors have examined the thermodynamic properties such as the inter-atomic separation and the bulk modulus of solids with different approximation and best-fit relations. It has become possible to compute with great accuracy an important number of structural and electronic properties of solids. The abolition calculations are complex and require significant effort. Therefore, more empirical approaches have been developed [12,13] to compute properties of materials. In many cases, the empirical methods offer the advantage of applicability to a broad class of materials and to illustrate trends. In many applications, these empirical approaches do not give highly accurate results for each specific material, but are still very useful.

Cohen [14] has established an empirical formula for calculation of the bulk modulus B; based on the nearest-neighbor distance. His result is in agreement with experimental values. Lam et al. [15] have derived an analytical expression for the bulk modulus from the total energy. This expression is different in structure from the empirical formula, but gives similar numerical results. Also, they have obtained an analytical expression for the pressure derivative B of the bulk modulus. The theory yields a formula with two attractive features. Only the lattice constant is required as input, the computation of B itself is trivial. Consideration of hypothetical structure and simulation of the experimental conditions is required to make practical use of this formula. The aim is to see how a qualitative concept, such as the bulk modulus, shear modulus, young's modulus and plane modulus can be related to the energy gap and porosity of PS. It was argued that the dominant effect is the degree of covalence characterized by Phillips homopolar gap Eh [16], and one reason for presenting these data in this work is that the validity of the calculations that is not restricted in computed space.

Among the most challenging characterization techniques of thin films, coating and bulk materials are ultrasonic nondestructive evaluation methods, involving the measurements of wave velocities. The acoustic parameters such as transverse, longitudinal and Rayleigh velocities (VT, VL and VR, respectively), longitudinal impedance, transverse impedance (ZL, ZT) and elastic constants can be

investigated through the following relation. The porosity determines the acoustic velocities v and density ρ in the sample, which together determine the acoustic impedance Z = ρv. The PS model is an isotropic two-component system, i.e., a silicon carcass and pores with the dimensions much less than the light wavelength λ. Consequently, PS can be treated as an optically isotropic medium with an effective refractive index n. Its n, which is a function of porosity, is higher than that of air and lower than that of silicon. We consider layers with a low extinction coefficient when the imaginary part of the complex refractive index can be Neglected. The two-component Bruggeman model is known to be in agreement with the experimental data for PS layers on low resistivity p+□Si substrates. This kind of model is based on additivity of contribution from each phase into effective polarizability of the medium.

2. RESULT AND DISCUSSION

2.1 Optical Properties

The energy gap determines the threshold for absorption of photons in semiconductors and its refractive index (n) is a measure of its transparency to incident spectral radiation. The 'n' is an important physical parameter related to microscopic atomic interactions. Theoretically, two different approaches in viewing this subject are the refractive index related to density, and the local polarizability of these entities [17]. On the other hand, the crystalline structure represented by a delocalized picture, refractive index will be closely related to the energy band structure of the material, complicated quantum mechanical analysis requirements and the obtained results.

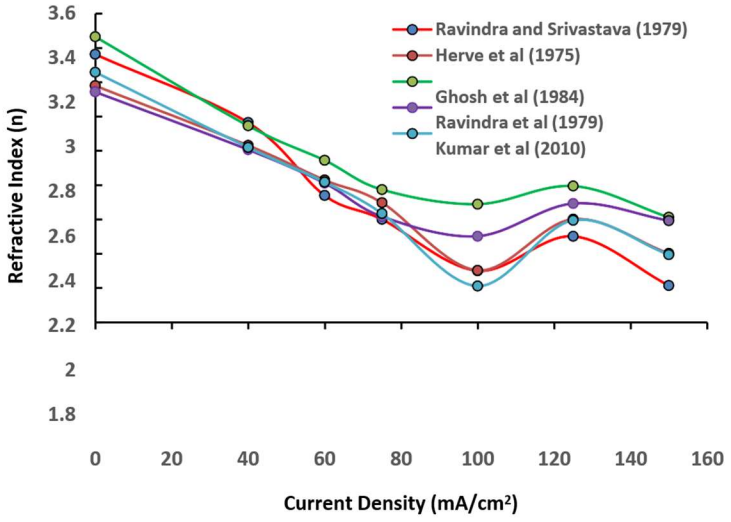

Fig. 1. Variation of refractive index (n) with current density forfive models.

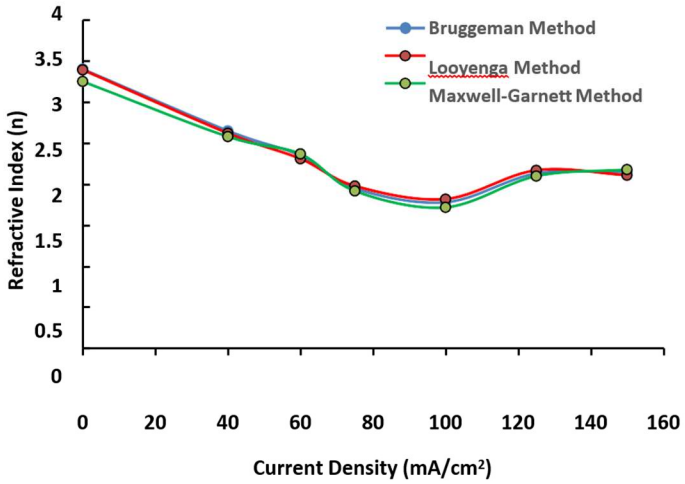

Fig. 2. Variation of refractive index (n) with current density for Effective medium model.

By using the five theoretical models and effective medium approximation methods, the 'n' and dielectric constant (ε) have been calculated for different current density, etching time and polymer concentrations as a function of the percentage of porosity and their results are illustrated in Fig. (1-23). The calculated 'n' and 'ε' of the bulk Si is in good accordance with experimental results. But these values are lower in PS samples [18].

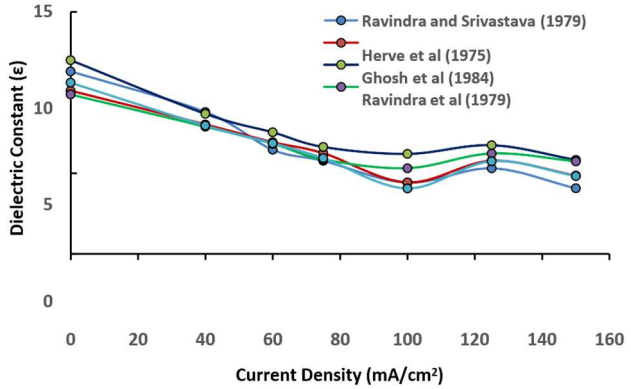

Fig. 3. Variation of dielectric constant (ε) with current density for five models.

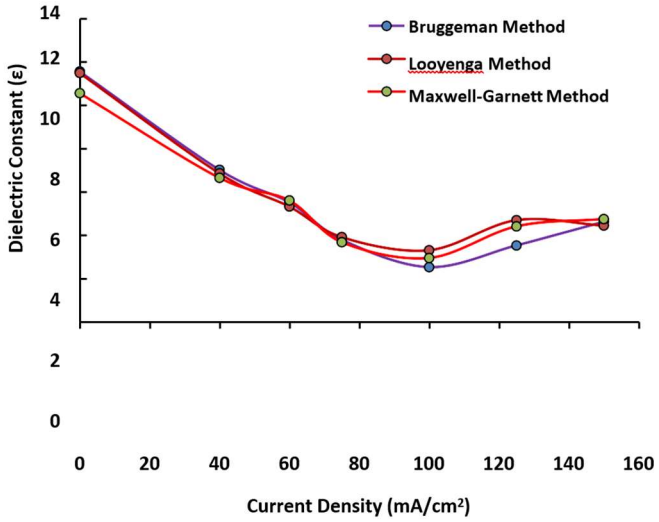

Fig. 4. Variation of dielectric constant (ε) with current density for Effective medium model.

When increase the percentage of porosity of PS, the both values of 'n' and 'ε' are found to be decrease with increase current density up to 100 mA/cm2 and 150 mA/cm2 while slightly increased at 125 mA/cm2. The noticeable changes in 'n' and 'ε' at 125 mA/cm2, is attributed to the pore formation occurring in the next layer of c-Si when the current density was fixed above 100 mA/cm2. The theoretical results are well matched with experimental results. Among the five methods and effective medium methods, the values 'n' and 'ε' derived from Ghose et al., [18] is in good accordance with experimental results.

Similar trends of results are arrived in the case of different etching time with fixed constant current density. As can be seen in the Table. 1 that 'n' and 'ε' decreases with increasing the etching time (10 – 40 min) and it slightly increases at 50 min etching. While it again decreased at 60 min etching indicating the pore formation occurring in the next c-Si wafer. The results of 'ε' also found to be similar trends to that of 'n'. The observed trends in 'n' and 'ε' in effect of etching time on c-Si holds good with the effect of current density on c-Si wafer.

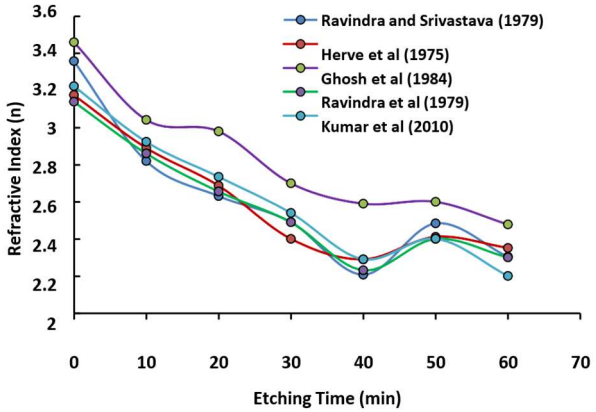

Fig. 5. Variation of refractive index (n)with etching time for five models.

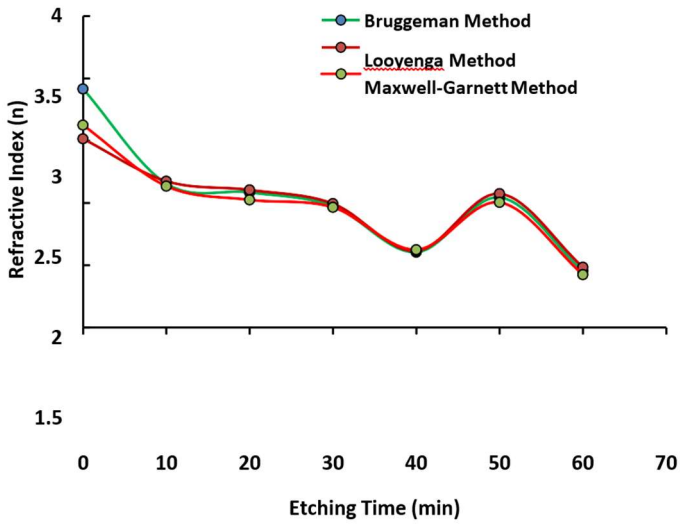

Fig. 6. Variation of refractive index (n) with etching time for Effective medium model.

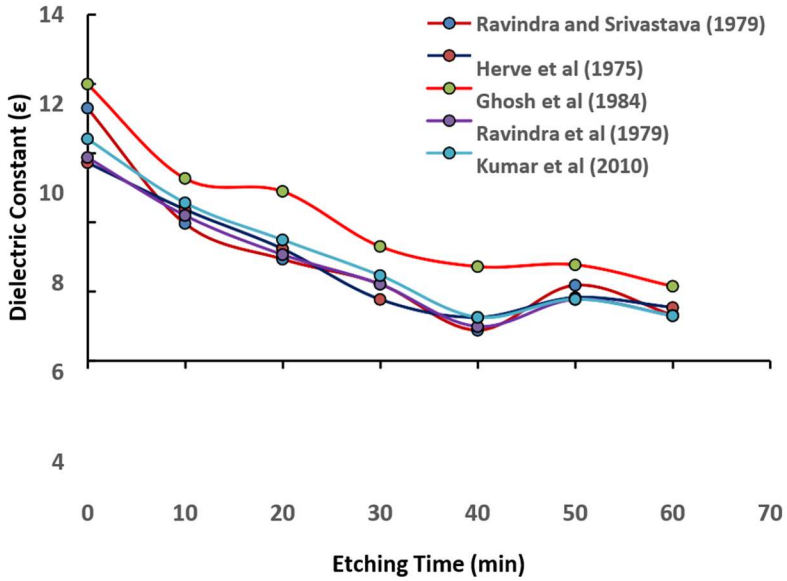

Fig. 7. Variation of dielectric constant (ε) with etching time for five models.

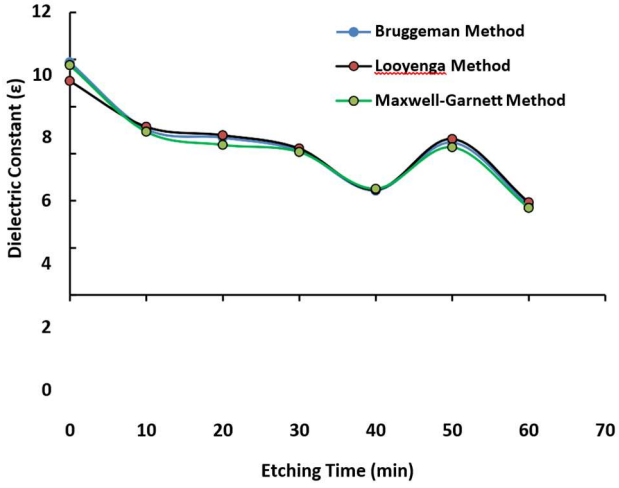

Fig. 8. Variation of dielectric constant (ε) with etching time for Effective medium model.

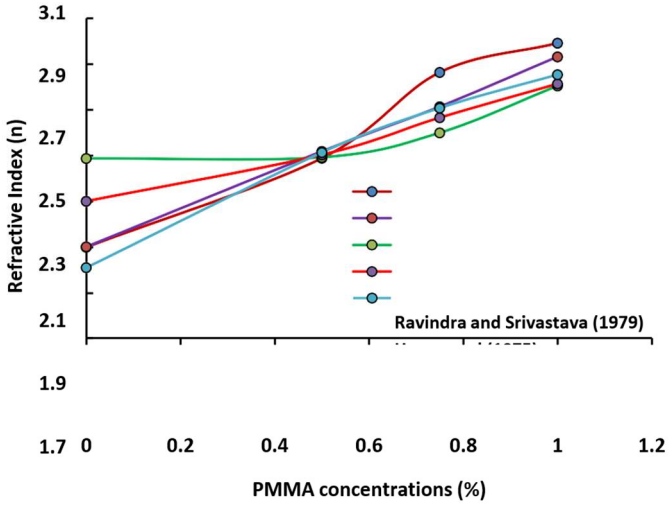

Fig. 9. Variation of refractive index (n) with current PMMA concentrations for five models.

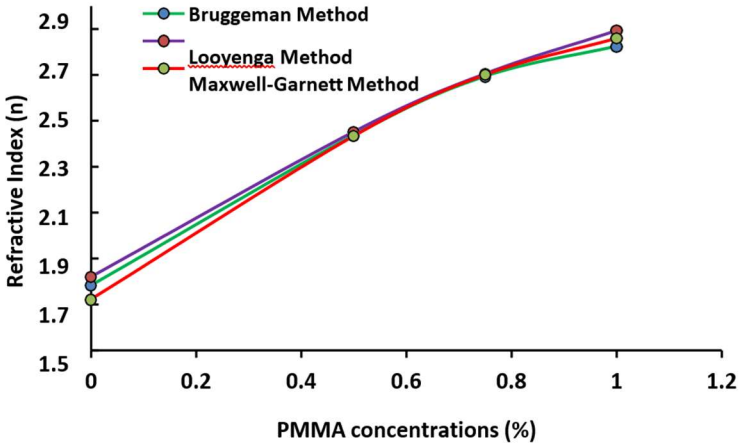

Fig. 10. Variation of refractive index (n) with current PMMA concentrations for Effective medium model.

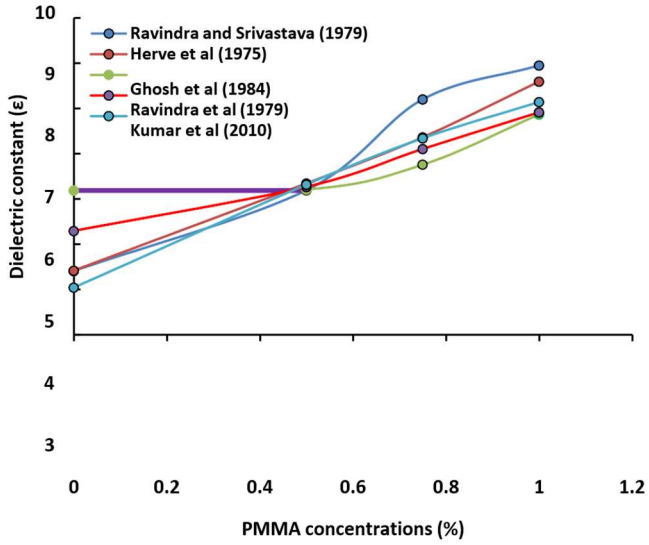

Fig. 11. Variation of dielectric constant (ε) with PMMA concentration for five models.

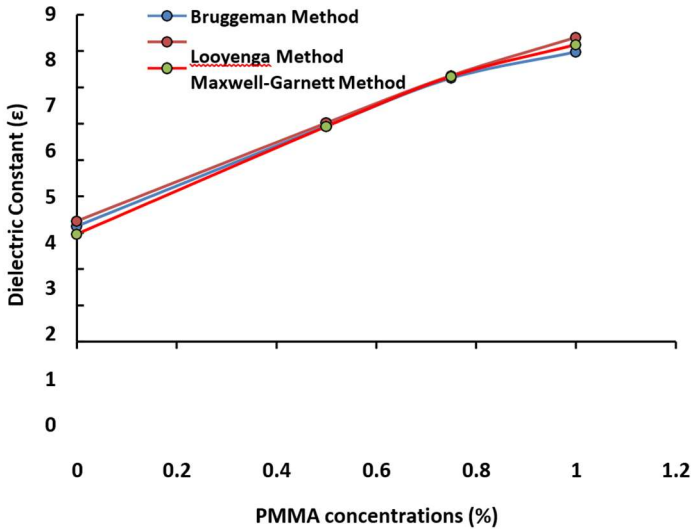

Fig. 12. Variation of dielectric constant (ε) with PMMA concentrations for Effective medium model.

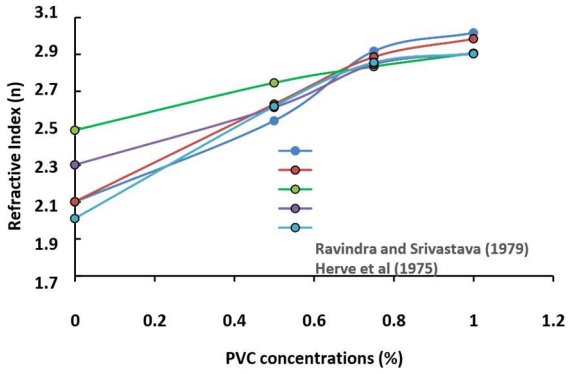

Fig. 13. Variation of refractive index (n) with PVC concentrations for five models.

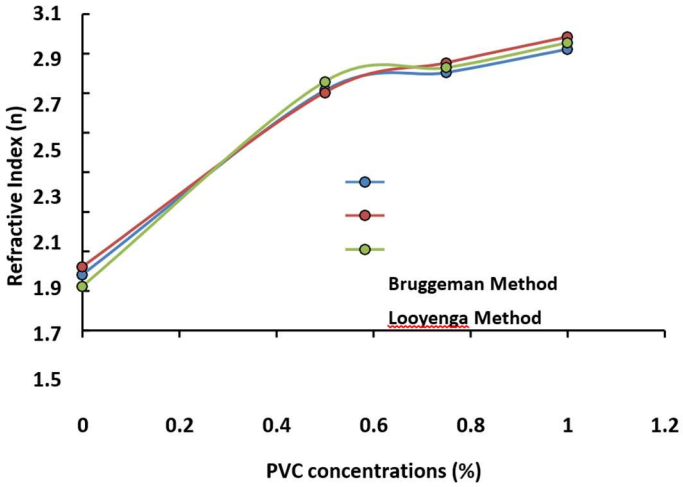

Fig. 14. Variation of refractive index (n) with PVC concentrations for Effective medium model.

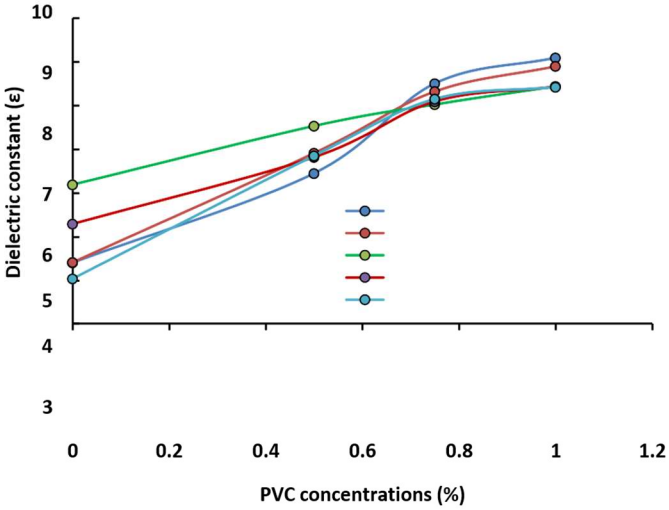

Fig. 15. Variation of dielectric constant (ε) with PVC concentrations for five models.

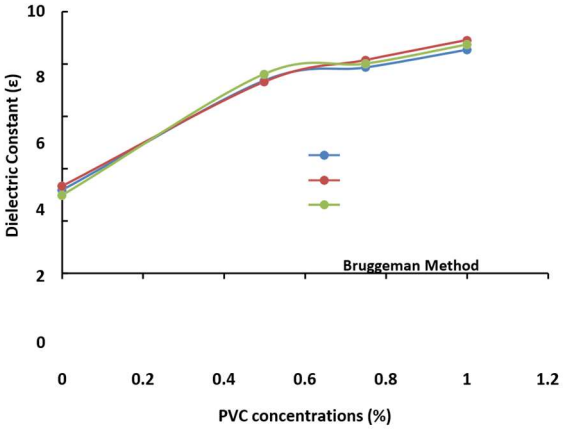

Fig. 16. Variation of dielectric constant (ε) with PVC concentration for Effective medium model.

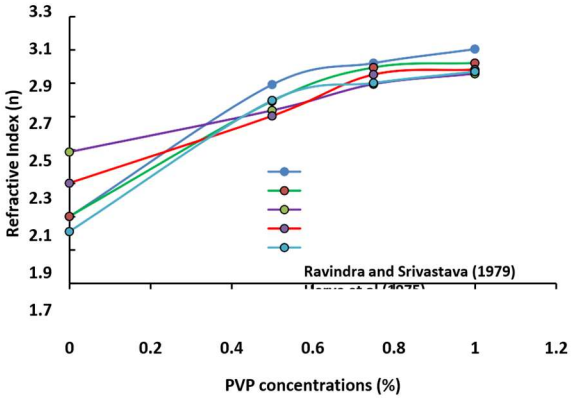

Fig. 17. Variation of refractive index (n) with PVC concentration for five models.

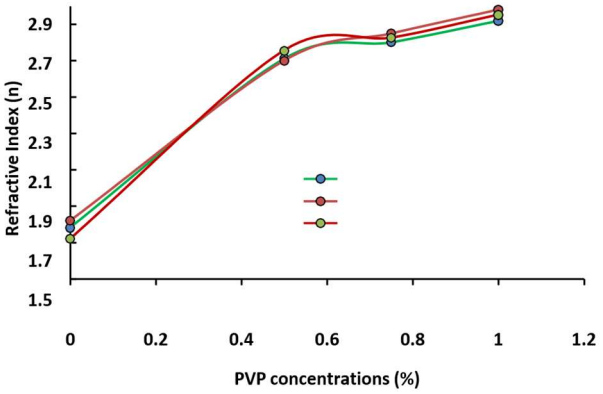

Fig. 18. Variation of refractive index (n) with PVP concentrations for Effective medium model.

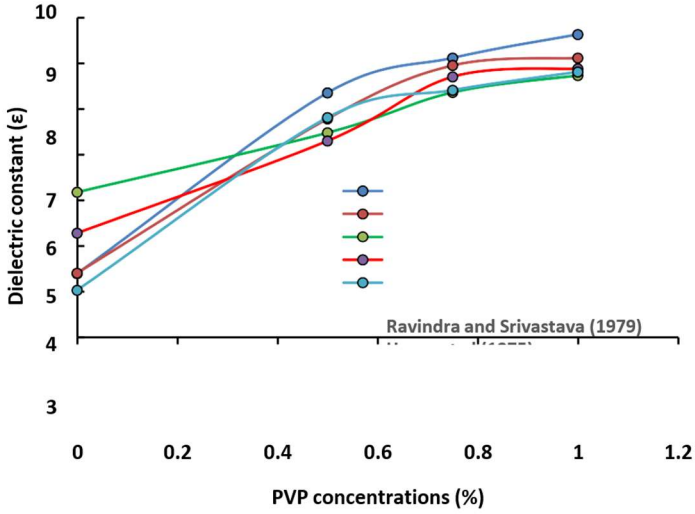

Fig. 19. Variation of dielectric constant (ε) with PVP concentrations for five models.

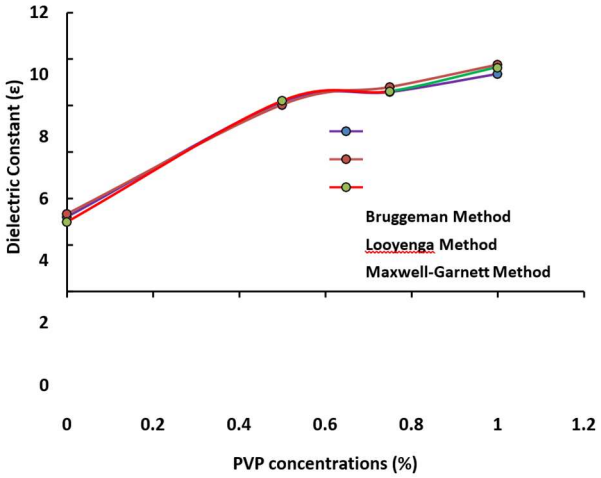

Fig. 20. Variation of dielectric constant (ε) with PVP concentration for Effective medium model.

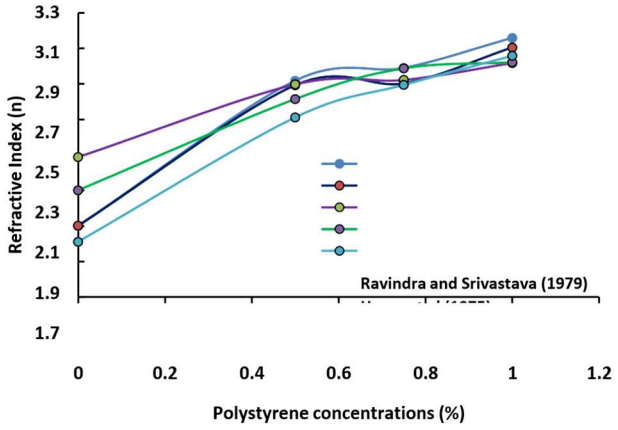

Fig. 21. Variation of refractive index (n) with polystyrene concentration for five models.

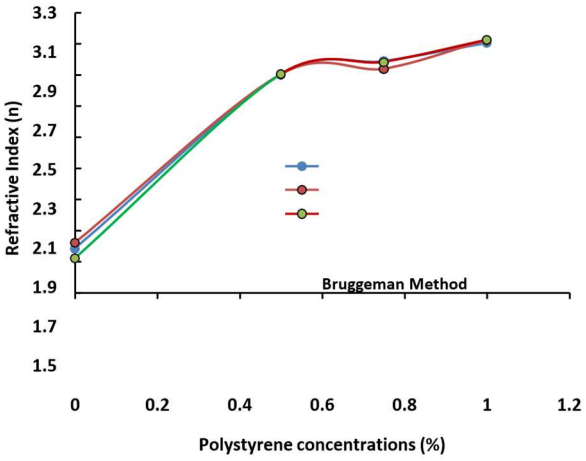

Fig. 22. Variation of refractive index (n) with polystyrene concentration for Effective medium model.

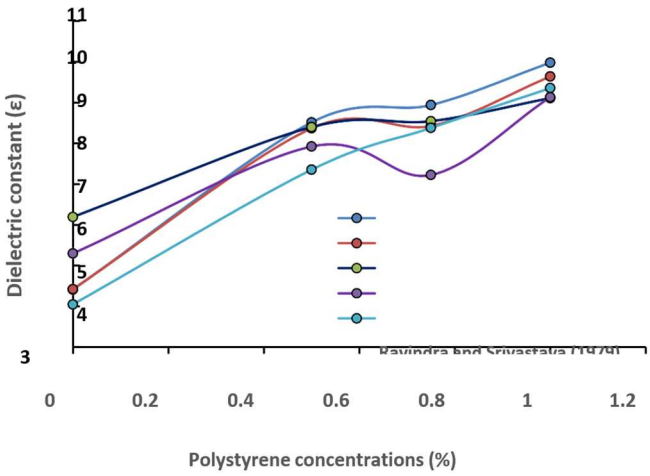

Fig. 23. Variation of dielectric constant (ε) with polystyrene concentration for five models.

In the case of polymers treated PS, the values of both 'n' and 'ε' are found to opposite trend to the effect of current density and etching time. The values of 'n' and 'ε' are found to be increasing with increase the polymer concentrations (0.5%, 0.75% and 1.0%) which are mainly due to decrease of porosity in the order of 63 to 36 % for PMMA, 55 to 32 % for PVC, 45 to 23 % for PVP and 38 to 18 % for polystyrene. The decrease of porosity in polymer treated PS samples are due to infiltration of polymer molecule in the pores as increase the layer thickness with the polymer concentrations. Among the four polymers, PMMA and PVC exhibited lower 'n' and 'ε' values as coincide well with the experimental values. In conclusion the theoretical results of 'n' and 'ε' are related to the percentage of porosities in the c-Si wafer as can be correlated with SEM and AFM analysis.

3. CONCLUSION

In conclusion, the study employed five theoretical models and the effective medium approximation methods to calculate the refractive index ('n') and dielectric constant ('ε') for varying current densities, etching times, and polymer concentrations in porous silicon (PS) samples. The results showed good agreement with experimental data for bulk silicon, but lower values were observed in PS samples, particularly as the percentage of porosity increased. When examining the impact of current density, it was observed that both 'n' and 'ε' decreased with increasing current density up to 100 mA/cm² and 150 mA/cm², with a slight increase at 125 mA/cm². This unique behavior at 125 mA/cm² was attributed to pore formation in the next layer of crystalline silicon (c-Si). These findings aligned well with experimental results, and the method by Ghose et al. yielded particularly accurate results.

A similar trend was observed when investigating different etching times while keeping the current density constant. 'n' and 'ε' decreased with increasing etching time (10–40 min), with a slight increase at 50 min etching. However, they decreased again at 60 min, indicating pore formation in the underlying c-Si wafer. These trends were consistent with the effects observed with varying

current density on c-Si. In the case of PS treated with polymers, 'n' and 'ε' exhibited an opposite trend to the effects of current density and etching time. Increasing polymer concentrations (0.5%, 0.75%, and 1.0%) led to higher 'n' and 'ε' values due to a decrease in porosity. This decrease in porosity resulted from the infiltration of polymer molecules into the pores, increasing the layer thickness with higher polymer concentrations. Among the tested polymers, PMMA and PVC demonstrated lower 'n' and 'ε' values, aligning closely with experimental values.

In summary, the theoretical results of 'n' and 'ε' were directly related to the percentage of porosity in the c-Si wafer. These findings were further supported by SEM and AFM analyses, providing valuable insights into the complex relationship between porosity, current density, etching time, and polymer concentration in porous silicon samples.

- The calculated refractive index ‘n’ and dielectric constant ‘ε’ of the bulk Si is in good accordance with experimental results. But these values are lower in PS samples.
- The noticeable changes in ‘n’ and ‘ε’ at 125 mA/cm2, is attributed to the pore formation occurring in the next layer of c-Si as well matched with experimental results.
- In the case of different etching time the ‘n’ and ‘ε’ values hold good with the effect of current density on c-Si wafer.
- The ‘n’ and ‘ε’ values of the polymer treated samples showed the opposite trend to the effect current density and etching time.
- The theoretical results of ‘n’ and ‘ε’ are related to the percentage of porosities in the c-Si wafer as can be correlated with SEM and AFM analysis.

4. REFERENCES

1. Nader. N and Hashim. M.R. J. Electrochem. Sci,. 7 (2012) 11513 – 11518.
2. Torres-Costa. V and Martin-Palma, R.J. J. Mater. Sci,. 45 (2010) 2823 – 2838.
3. Doghmane. A, Hadjoub. Z, Doghmane. M and Hadjoub, F. Quantum Electron Optoelectron. 9 (2006) 4 – 11.
4. Da Fonseca. R. J, Saurel, J.M, Foucaran. S, camassel. J, Massone. E, taliercio. T, and Boumaiza. Y. J. Mater. Sci., 30 (1995) 35 – 39.
5. Gupta, V.P, and Ravindra, N.M. Phys. Status Solidi B, 100 (1980) 715 – 719.
6. Reddy, R.R, Anjaneyulu. S, and Samara. C.L.N. J. Phys. Chem. Solids. 54 (1993) 635 – 637
7. Ravindra. N.M. and Srivastava. V.K. Phys. Status Solidi B, 93 (1979) 155 – 160.
8. Kumar. V, and Singh. J.K, Indian J. Pure Appl. Phys., 48 (2010) 571 – 574.
9. A.M. Sherry, M. Kumar. J. Phys. Chem. Solids. 52 (1991) 1145.
10. J.L. Tallon. J. Phys. Chem. Solids. 41 (1980) 837.
11. M. Kumar. Physica B. 205 (1995) 175.
12. M. Kumar, S.P. Upadhyaya. Phys. Stat. Sol. (b). 181 (1994) 55.
13. J.C. Phillips, Bonds and Bands in Semiconductors, Academic Press. San Diego, 1973.
14. W.A. Harison, Electronic Structure and the Properties of Solids, General Publishing Company, Toronto, 1973.

15. R.K. Pandey. J. Phys. Chem. Solids. 59 (1998) 1157.
16. Da Fonseca, R.J.M., Saurel, J.M., Foucaran, S., Camassel, J., Massone, E., Taliercio, T., and Boumaiza, Y., J. Mater. Sci., 30 (1995) 35 – 39.
17. N.M. Balzaretti, J.A.H. da Jornada, Solid State Commun. 99 (1996) 943.
18. Ravindra. N.M, and Srivastava. V.K. Infrared Phys. 19 (1979) 603 – 604.